

Endoplasmic Reticulum Stress Induces the Early Appearance of Pro-apoptotic and Anti-apoptotic Proteins in Neurons of Five Familial Alzheimer's Disease Mice

Hui Shen^{1,2}, Xiao-Dong Pan^{1,2}, Jing Zhang^{1,2}, Yu-Qi Zeng^{1,2}, Meng Zhou^{1,2}, Lu-Meng Yang^{1,2}, Bing Ye^{1,2}, Xiao-Man Dai^{1,2}, Yuan-Gui Zhu^{1,2}, Xiao-Chun Chen^{1,2}

¹Department of Neurology and Geriatrics, Fujian Institute of Geriatrics, Fujian Medical University Union Hospital, Fuzhou, Fujian 350001, China

²Key Laboratory of Brain Aging and Neurodegenerative Diseases, Fujian Key Laboratory of Molecular Neurology, Fujian Medical University, Fuzhou, Fujian 350001, China

Abstract

Background: Amyloid β ($A\beta$) deposits and the endoplasmic reticulum stress (ERS) are both well established in the development and progression of Alzheimer's disease (AD). However, the mechanism and role of $A\beta$ -induced ERS in AD-associated pathological progression remain to be elucidated.

Methods: The five familial AD (5 \times FAD) mice and wild-type (WT) mice aged 2, 7, and 12 months were used in the present study. Morris water maze test was used to evaluate their cognitive performance. Immunofluorescence and Western blot analyses were used to examine the dynamic changes of pro-apoptotic (CCAAT/enhancer-binding protein homologous protein [CHOP] and cleaved caspase-12) and anti-apoptotic factors (chaperone glucose-regulated protein [GRP] 78 and endoplasmic reticulum-associated protein degradation-associated ubiquitin ligase synovial apoptosis inhibitor 1 [SYVN1]) in the ERS-associated unfolded protein response (UPR) pathway.

Results: Compared with age-matched WT mice, 5 \times FAD mice showed higher cleaved caspase-3, lower neuron-positive staining at the age of 12 months, but earlier cognitive deficit at the age of 7 months (all $P < 0.05$). Interestingly, for 2-month-old 5 \times FAD mice, the related proteins involved in the ERS-associated UPR pathway, including CHOP, cleaved caspase-12, GRP 78, and SYVN1, were significantly increased when compared with those in age-matched WT mice (all $P < 0.05$). Moreover, ERS occurred mainly in neurons, not in astrocytes.

Conclusions: These findings suggest that compared with those of age-matched WT mice, ERS-associated pro-apoptotic and anti-apoptotic proteins are upregulated in 2-month-old 5 \times FAD mice, consistent with intracellular $A\beta$ aggregation in neurons.

Key words: Alzheimer's Disease; Amyloid β ; Apoptosis; Endoplasmic Reticulum Stress; Unfolded Protein Response Pathway

INTRODUCTION

Alzheimer's disease (AD) is a common neurodegenerative disease in the central nervous system. The pathological features of AD include senile plaques formed by extracellular amyloid β ($A\beta$) aggregation, neurofibrillary tangles formed by abnormal accumulation of hyperphosphorylated tau protein, synaptic impairments, and neuronal loss in the cerebral cortex and hippocampus. $A\beta$ aggregation in the brain is central to the pathological changes of AD and leads to a series of pathological events, which further promote $A\beta$ aggregation, resulting in cascade amplification.^[1]

The endoplasmic reticulum (ER), a dynamic membranous organelle, is involved in protein synthesis, posttranslational modification, folding, calcium storage, lipid metabolism, and

steroid hormone synthesis. Specific stress conditions such as hyperglycemia, hyperlipidemia, hypoxia, chemical toxicants, and genetic mutations can induce the accumulation of unfolded or misfolded proteins in the ER and changes in ER

Address for correspondence: Prof. Xiao-Chun Chen, Department of Neurology and Geriatrics, Fujian Institute of Geriatrics, Fujian Medical University Union Hospital, Fuzhou, Fujian 350001, China
Key Laboratory of Brain Aging and Neurodegenerative Diseases, Fujian Key Laboratory of Molecular Neurology, Fujian Medical University, Fuzhou 350001, China
E-Mail: chenxc998@163.com

This is an open access article distributed under the terms of the Creative Commons Attribution-NonCommercial-ShareAlike 3.0 License, which allows others to remix, tweak, and build upon the work non-commercially, as long as the author is credited and the new creations are licensed under the identical terms.

For reprints contact: reprints@medknow.com

© 2016 Chinese Medical Journal | Produced by Wolters Kluwer - Medknow

Received: 03-08-2016 **Edited by:** Qiang Shi

How to cite this article: Shen H, Pan XD, Zhang J, Zeng YQ, Zhou M, Yang LM, Ye B, Dai XM, Zhu YG, Chen XC. Endoplasmic Reticulum Stress Induces the Early Appearance of Pro-apoptotic and Anti-apoptotic Proteins in Neurons of Five Familial Alzheimer's Disease Mice. Chin Med J 2016;129:2845-52.

Access this article online

Quick Response Code:



Website:
www.cmj.org

DOI:
10.4103/0366-6999.194643

functions, resulting in endoplasmic reticulum stress (ERS). In turn, ERS stimulates the unfolded protein response (UPR) and restores cellular homeostasis while sustained ERS leads to cell apoptosis.^[2-4] Many studies have shown that ERS is involved in the development and progression of neurodegenerative diseases such as AD, Parkinson's disease, Huntington's disease, and amyotrophic lateral sclerosis^[5] although the underlying mechanisms still remain blurred.

The activation of the UPR pathway requires the activation of three sensor proteins: inositol-requiring enzyme 1 (IRE-1), activating transcription factor 6 (ATF6), and protein kinase RNA-like ER kinase.^[6,7] These sensors serve to promote the expression of chaperone protein, glucose-regulated protein (GRP) 78, to repair misfolded or unfolded proteins, to accelerate ER-associated protein degradation (ERAD),^[8] and to aggravate the phosphorylation of eukaryotic translation initiation factor 2 α . This reduces protein translation and ER load to restore protein homeostasis and protect cells. Sustained ERS induces the activation of the ER-specific apoptosis pathway by promoting the expression of the transcriptional activator CCAAT/enhancer-binding protein homologous protein (CHOP) and caspase-12 activation.^[9] Activated IRE-1 interacts with tumor necrosis factor receptor-associated factor 2 (TRAF2) and apoptosis signal-regulating kinase 1 (ASK1) via the cytosolic enzyme domain to form IRE-1-TRAF2-ASK1 complexes, which in turn stimulate the c-Jun amino-terminal kinase (JNK) pathway to promote cell apoptosis, thus preventing the damaging impact of misfolded and secreted proteins on tissues and organisms.

Genetic mutations in AD lead to A β overexpression in the brain and subsequent neurotoxicity, which leads to pathogenesis. The five familial Alzheimer's disease (5 \times FAD) mice were established by overexpressing the five familial-inherited AD mutant genes (APP K670N/M671L [Sweden]+I716V [Florida] +V717I [London]+PS1 M146L+L286V) under the control of the neuron-specific Thy-1 promoter. This mouse model is characterized by many pathological features similar to AD, including amyloid plaque deposition, gliosis, neuronal degeneration, neuronal loss, and cognitive deficits at the age of 4–5 months. More importantly, this mouse model has been documented to show the earliest signs of intracellular A β aggregation in neurons in 1.5-month-old mice, which indicates these mice as a suitable candidate to investigate the early events of AD.^[10]

In this study, we investigated the time-ordered changes of pro-apoptotic and anti-apoptotic factors to determine the role of the UPR signaling pathway in cognitive decline of 5 \times FAD mice. The outcome may clarify the role of ERS in the pathological progression of AD.

METHODS

Animal feeding and grouping

The 5 \times FAD APP/PS1 transgenic B6/SJL mice with five familial inherited AD mutant genes (APP K670N/M671L [Sweden]+I716V [Florida]+V717I [London]+PS1

M146L+L286V) under the control of the neuron-specific Thy-1 promoter and wild-type (WT) B6/SJL mice with the identical genetic background were provided by Prof. Marry Jo Ladu (Department of Anatomy and Cell Biology, University of Illinois at Chicago, USA). Experimental animals were housed in a pathogen-free colony (IVC System, Tecniplast, Italy) and allowed free access to food and water. They were raised, 4–5 animals/cage, under 12-h light/12-h dark conditions at 22°C–25°C with a humidity of 50–60%. All protocols and procedures used in this study were approved by the Institutional Animal Care and Use Committee at Fujian Medical University in compliance with the US National Institutes of Health "Guidelines for the Care and Use of Laboratory Animals". The 5 \times FAD transgenic and WT mice at 2, 7, or 12 months of age were used for subsequent experiments with 10–14 animals per group ($n = 12$ in each 2-month-old group, $n = 10$ in each 7-month-old group, $n = 10$ in the 12-month-old WT group, and $n = 14$ in the 12-month-old 5 \times FAD group).

Behavior analysis

Morris water maze tests were performed as described previously.^[11] The swimming behavior of mice was evaluated four times a day for 5 days. The swimming trace was monitored by camera and analyzed with SMART 2.0 software (PanLab, Barcelona, Spain). The escape latency(s) and number of crossings over a hidden platform in 60 s were recorded.

Immunohistochemistry

Mice were anesthetized using 10% chloral hydrate by intraperitoneal injection (3 ml/kg). Then, left ventricular perfusion was performed and brain tissues were isolated quickly on ice. Brain tissues were cut along the central sagittal suture, and the left hemisphere was fixed in 4% paraformaldehyde/0.1 mol/L phosphate-buffered saline (pH 7.4) at 4°C for 24 h, followed by dehydration in 30% sucrose buffer for 48–72 h. The brain tissues were then embedded and cut into 30 μ m cortical slices using a freezing microtome (CM1850, Leica, Wetzlar, Germany) and stored at –20°C. Immunohistochemistry was performed as follows:^[10] brain slices were washed with Tris-buffered saline (TBS) and treated with 10% hydrogen peroxide at room temperature for 10 min to diminish endogenous catalase activity. The brain slices were then blocked with a buffer (containing 5% goat serum [GS], 0.25% bovine serum albumin [BSA], 0.3% Triton X-100, TBS) at room temperature for 1 h. Primary antibodies 6E10 (1:8000, Covance, Princeton, NJ, USA) and NeuN (1:4000, Abcam, Cambridge, UK) were diluted in a buffer (containing 2% GS, 0.25% BSA, 0.3% Triton X-100, TBS) and incubated at 4°C overnight. Biotin-labeled secondary antibodies anti-mouse IgG (1:600) and anti-rabbit IgG (1:400) (Vector Laboratories, Burlingame, CA, USA) were added subsequently and incubated at room temperature for 1.5 h. 3,3'-diaminobenzidine staining was employed, and slices were air-dried at room temperature overnight. The slices were then hydrated for 5 min, dehydrated

using an ethanol gradient, treated with xylene, and finally mounted with neutral balsam. The slices were imaged using a microscopy (Leica DM 4000B, Germany), and image acquisition was performed with Image-Pro Express 5.1 image analysis software (Media Cybernetics, Rockville, MD, USA). For quantitative analysis, 6 mice were randomly selected from each group and 3 consecutive sections of each mouse were measured. The prefrontal cortex region was selected as regions of interest, and the identical area within the measuring frame in a 10× objective lens was labeled. The number of neurons in the frame was counted by 40× magnification. The clear brown cellular boundaries were considered positive although positive cells outside the frame were rejected. “Cells” that were lightly stained or had irregular shapes were excluded from quantification. Then, the mean value for each mouse was calculated.

Immunocytochemistry

Brain slices were washed with TBS buffer and blocked with a specific buffer (containing 5% donkey serum [DS], 0.25% BSA, 0.3% Triton X-100, TBS) at room temperature for 1 h. The primary antibodies (diluted in 2% DS, 0.25% BSA, 0.3% Triton X-100, TBS) used were: 6E10, GRP 78 (1:50, Santa Cruz, CA, USA), CHOP (1:50, Santa Cruz), glial fibrillary acidic protein (GFAP) (1:4000, Millipore, Boston, USA), and β -III-tubulin (1:4000, Abcam). The 6E10 was co-incubated with GRP 78, CHOP, GFAP, and tubulin primary antibodies. GRP 78 or CHOP was incubated with GFAP and β -III-tubulin. Primary antibodies were added and incubated at 4°C overnight. Alexa Fluor 488- or 594-conjugated donkey anti-mouse or anti-rabbit IgG (1:1500, Invitrogen, Carlsbad, CA, USA) were then added and incubated at room temperature in the dark for 1.5 h. The 4',6-diamidino-2-phenylindole (DAPI) (diluted by 1:8000 in H₂O) was then added and incubated for 5 min. ProLong Gold antifade reagent (Invitrogen) was used for slice mounting, and slices were imaged using confocal microscopy (Leica TCS SP5, Leica Microsystems Wetzlar GmbH, Germany).

Western blots

Isolated mouse cortical tissues were added into tissue lysates (1% Triton X-100, 50 mmol/L sodium fluoride, 2 mmol/L sodium orthovanadate, 10 mmol/L β -sodium glycerophosphate, 10 mmol/L sodium pyrophosphate, 1% protease inhibitor cocktail [p8340, Sigma-Aldrich, St. Louis, MO, USA] dissolved in TBS buffer, pH 7.4) at a ratio of 1:10 (mg/ml). The mixture was incubated on ice for 30 min, and lysis was performed using the ultrasound method. The lysates were centrifuged at 16,000 ×g at 4°C for 25 min. Supernatants were collected and proteins were separated by sodium dodecyl sulfate polyacrylamide gel electrophoresis (SDS-PAGE). Subsequently, the proteins were transferred to polyvinylidene fluoride (PVDF) membranes and blocked with 3% nonfat milk or 5% BSA in TBST buffer at room temperature for 2 h. The membranes were incubated at 4°C overnight with the following primary antibodies: GRP 78 (1:200), CHOP (1:500), SAPK/JNK (1:1000, Cell Signaling, Boston, USA), p-SAPK/JNK (Thr183/Tyr185) (1:1000, Cell Signaling), caspase-12 (1:500,

Cell Signaling), cleaved caspase-3 (1:500, Cell Signaling), SYVN1 (1:2000, Abcam), β -actin (1:2000, Abcam), and β -III tubulin (1:100,000). Horseradish peroxidase-labeled goat anti-rabbit or anti-mouse IgGs (1:2000) were subsequently added and incubated at 37°C for 1.5 h. ImageJ software (National Institutes of Health, Bethesda, MA, USA) was used for quantitative analysis.

Statistical analysis

Quantitative data were expressed as the mean \pm standard error (SE) and analyzed with the GraphPad Prism 6.01 software package (GraphPad, San Diego, CA, USA). Escape latency in the behavior analysis was performed using a repeated-measure multiway analysis of variance (ANOVA) while other data were evaluated using two-way ANOVA. If the main effects and the interaction were significant, the genotypes were compared by Student's *t*-test, or multiple conditions among the same genotype were evaluated with one-way ANOVA. Multiple comparisons were analyzed by Bonferroni *post hoc* test. A value of $P < 0.05$ was considered statistically significant.

RESULTS

Increased amyloid β induces the declined cognition in 7-month-old five familial Alzheimer's disease mice and the loss of neurons in the frontal cortex of the 12-month-old ones

To investigate cognitive changes, we tested mice's behavioral performance in the Morris water maze. We found that compared with age-matched WT mice, 7- and 12-month-old 5×FAD mice displayed a prolonged escape latency ($F = 14.710$, $P < 0.01$ for 7-month-old; $F = 5.939$, $P < 0.05$ for 12-month-old), indicating an obvious decline in learning ability and memory retention. In the probe trial, when the platform was removed, the 7- and 12-month-old 5×FAD mice crossed significantly less over the location of the removed platform than age-matched WT mice ($t = 2.331$, $P < 0.05$ for 7-month-old; $t = 2.075$, $P < 0.05$ for 12-month-old) [Figure 1a]. Immunohistochemical analysis showed that A β was mainly localized in pyramidal neurons situated deep within the fifth layer of the cortex in 2-month-old mice. A β accumulation was increased in the brain tissues of 7-month-old mice and amyloid plaque deposition appeared around neurons secreting A β . In 12-month-old mice, a large amount of plaque deposition was observed in the brain tissues [Figure 1b]. Furthermore, we examined cleaved caspase-3 (the activated form), an executor molecule, in the apoptotic cascade by Western blots. Levels of cleaved caspase-3 in 5×FAD mice were increased in a time-dependent manner. Cleaved caspase-3 levels of 5×FAD mice were higher than those of WT mice at all-time points. The increase was significant at the age of 12 months ($n = 8$, $t = 2.504$, $P < 0.05$) [Figure 1c]. The number of neuron-positive staining in 12-month-old 5×FAD decreased in the fifth layer of the cortex when compared with that of the age-matched WT mice, indicating neuronal loss in 5×FAD mice ($n = 6$, $t = 2.987$, $P < 0.05$) [Figure 1d and 1e].

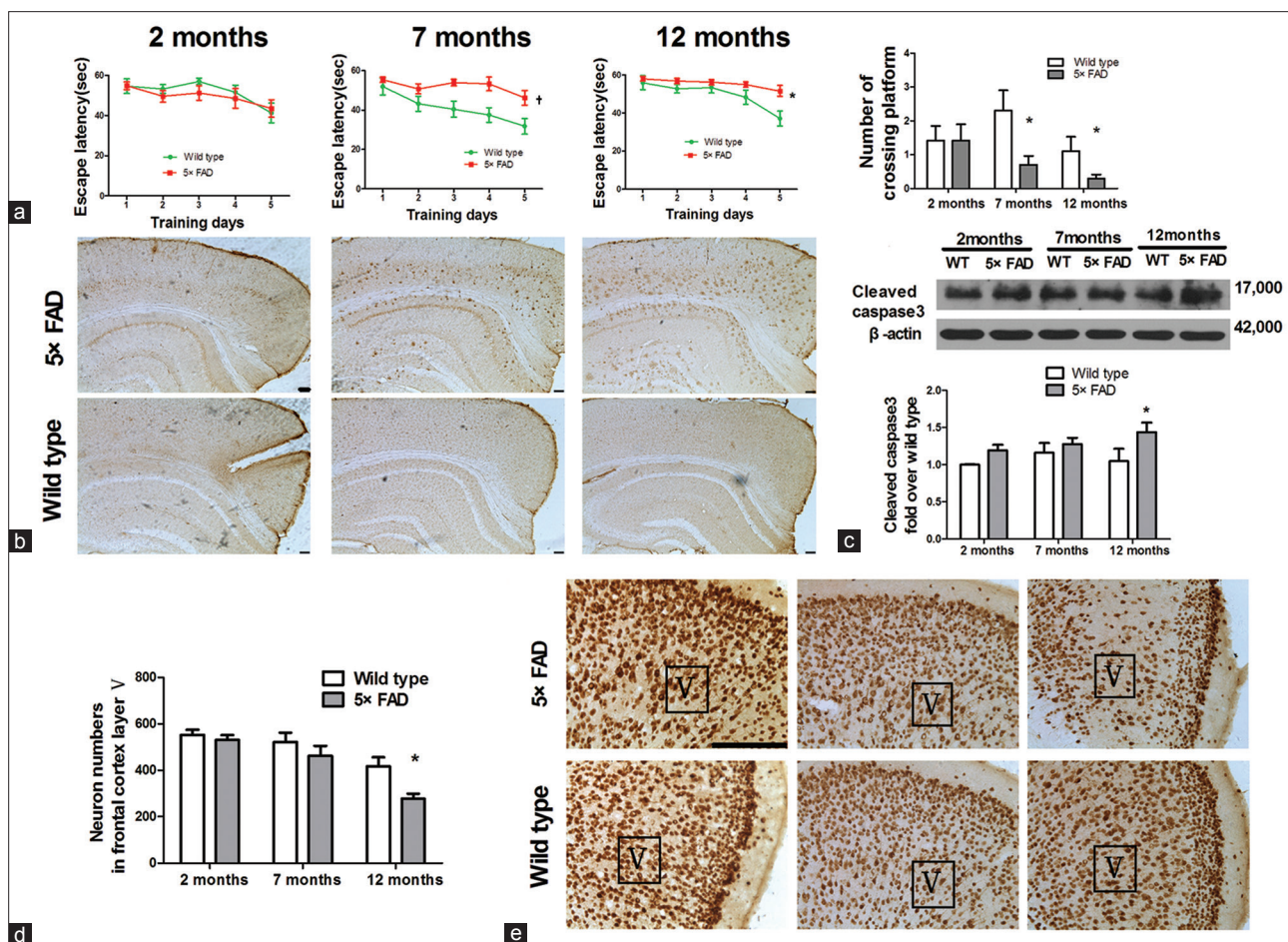


Figure 1: The declined cognition in 7-month-old 5×FAD mice and the loss of neurons in the frontal cortex of the 12-month-old ones. (a) Morris water maze test. Escape latency and the number of crossings over the platform in 7- and 12-month old 5×FAD mice ($n = 10-14$, $*P < 0.05$, $^{\dagger}P < 0.01$ vs. age-matched wild-type mice). (b) 6E10 staining in 2-, 7-, and 12-month-old 5×FAD mice and wild-type mice. Scale bar = 100 μm . (c) Western blots analysis showed that activated caspase-3 increased in 5×FAD mice at 12 months of age ($n = 8$, $*P < 0.05$ vs. wild-type mice). (d) The neurons within the fifth layer of the cortex was quantified ($n = 6$, $*P < 0.05$ vs. wild-type mice). (e) NeuN staining for neural nuclei in the frontal cortical slices from 2-, 7-, and 12-month-old mice. Scale bar = 100 μm ; 5×FAD: Transgenic mice with five familial Alzheimer's disease; WT: Wild-type mice; A β : Amyloid β ; V: The fifth layer of the frontal cortex.

Anti-apoptotic factors, glucose-regulated protein 78 and SYVN1, are significantly upregulated in 2-month-old five familial Alzheimer's disease mice

GRP 78 is a chaperone specifically localized in the ER, whose expression increases in response to ERS and serves as an ER-specific marker.^[6] In wild mice, GRP 78 expression increased insignificantly from the age of 2–7 months. In 5×FAD mice, GRP 78 expression decreased from the age of 2 to 12 months ($n = 6$, $t = 5.629$, $P < 0.01$ for 12 vs. 2 months). Interestingly, at the age of 2 months, GRP 78 expression in 5×FAD mice was significantly higher than that in age-matched WT mice ($n = 6$, $t = 2.549$, $P < 0.05$) [Figure 2a]. The GRP 78 expression was further detected by immunofluorescence. GRP 78 expression (stained green) in WT mice increased gradually from the age of 2–12 months. In 2-month-old 5×FAD mice, GRP 78 expression was higher than that of age-matched WT mice in the fifth layer of the cortex [Figure 2c]. Furthermore, GRP 78 staining was localized mainly in the staining of β -III tubulin (red), not in the staining of GFAP (red). Meanwhile, the distribution of A β and GRP 78 staining (red) was localized

totally with the 6E10 staining (green), as shown in Figure 2d. These data indicate that GRP 78 is expressed mainly in neurons, not in astrocytes.

SYVN1, a component of the ERAD pathway, is involved in the degradation of abnormal proteins to reduce ERS-induced apoptosis. At the age of 7 months and 12 months, no significant difference in SYVN1 expression was observed between 5×FAD mice and WT mice. However, at the age of 2 months, SYVN1 expression in 5×FAD mice was obviously higher than that in age-matched WT mice ($n = 5$, $t = 2.000$, $P < 0.05$) [Figure 2b].

Pro-apoptotic factors, CHOP and cleaved caspase-12, are significantly increased in five familial Alzheimer's disease mice

Although CHOP is rarely expressed in normal neurons, its expression can be increased by ERS to promote ER-specific apoptosis.^[12] In the current study, Western blots analysis revealed that CHOP expression increased with age in both WT mice and 5×FAD mice ($n = 7$, $t = 2.806$, $P < 0.05$ for

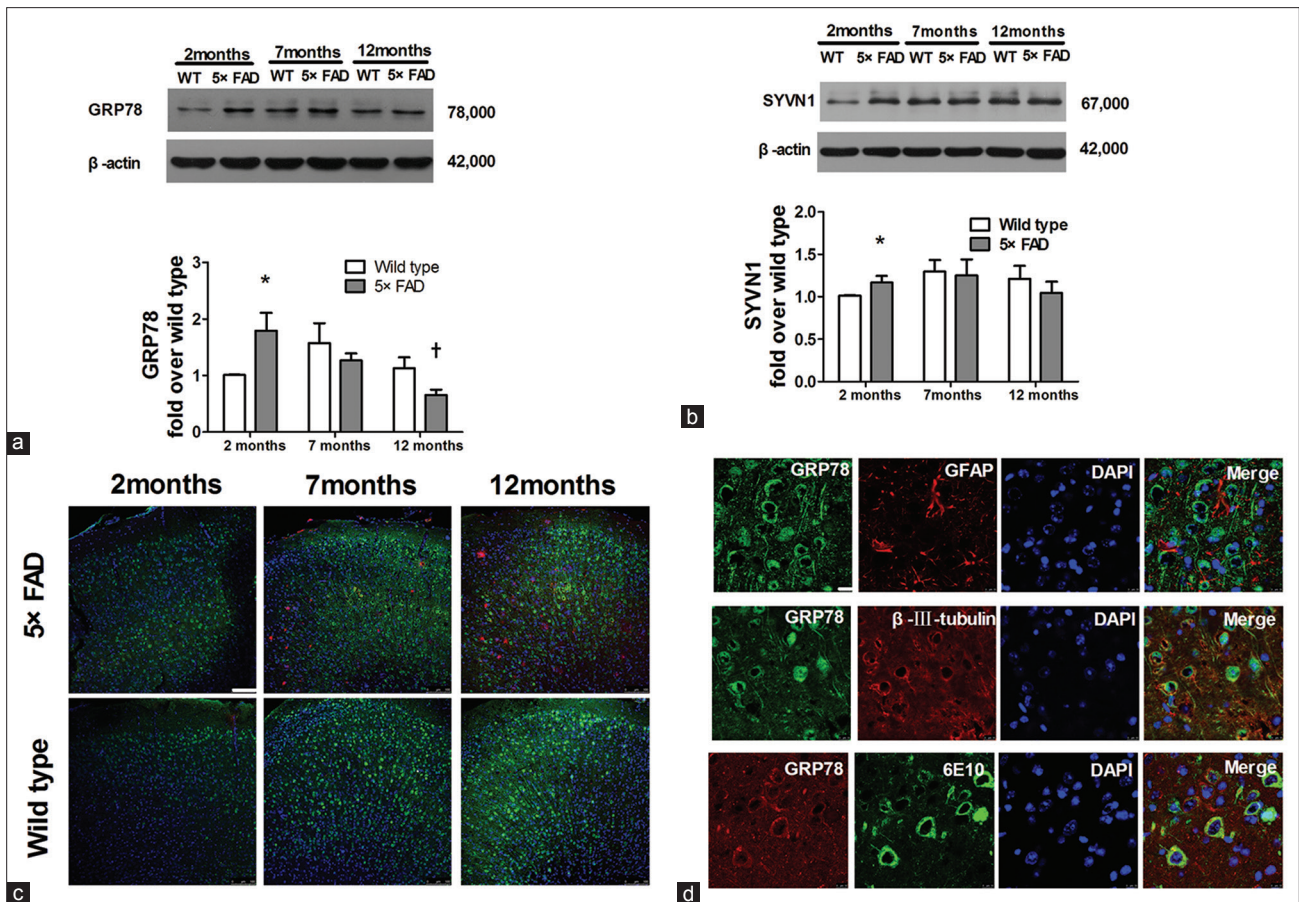


Figure 2: Significant upregulation of anti-apoptotic factors, GRP 78 and SYVN1, in 2-month-old 5×FAD mice. (a) GRP 78 expression of 5×FAD mice and age-matched WT mice at 2, 7, and 12 months old ($n = 6$, $*P < 0.05$ vs. 2-month-old WT mice; $†P < 0.01$ vs. 2-month-old 5×FAD mice). (b) SYVN1 expression of 5×FAD mice and age-matched WT mice at 2, 7, and 12 months old ($n = 5$, $*P < 0.05$ vs. 2-month-old WT mice). (c) Confocal images of GRP 78 (green), 6E10 (A β , red) and nuclei (DAPI, blue) in the cortical slices of 2-, 7- and 12-month-old mice by immunofluorescence staining. Scale bar = 100 μ m. (d) Confocal images of GRP 78 (green), GFAP (red) or β -III-tubulin (red) in the frontal cortical slices of 7-month-old 5×FAD mice by immunofluorescent staining. The bottom row of (d) indicates the immunofluorescent staining of GRP 78 (red) and 6E10 (green, targeting A β). Scale bar = 10 μ m. 5×FAD: Transgenic mice with five familial Alzheimer's disease; WT: Wild-type mice; GRP 78: Glucose-regulated protein 78; SYVN1: Ubiquitin ligase synovial apoptosis inhibitor 1; A β : Amyloid β ; 6E10: The antibody targeting A β ; GFAP: Glial fibrillary acidic protein; DAPI: 6-diamidino-2-phenylindole.

12-month-old WT mice vs. 2-month-old WT mice). Of note, compared with age-matched WT mice, CHOP expression increased significantly in 2-month-old 5×FAD mice ($n = 7$, $t = 2.322$, $P < 0.05$) [Figure 3a]. The CHOP expression was further detected by immunofluorescence and the CHOP staining (red) showed the same changing trend as that of the Western blots assay [Figure 3d]. Punctate distribution of CHOP in the cytoplasm and nucleus indicated CHOP activation, which serves as a transcription factor. Furthermore, CHOP staining (green) was localized mainly in the staining of β -III tubulin (red), not in the staining of GFAP (red). Meanwhile, CHOP staining (red) was localized totally with the 6E10 staining (green), as shown in Figure 3e. These data indicate that CHOP is predominantly expressed in 6E10-positive neurons, not in astrocytes. We further investigated the cleaved caspase-12 level by Western blots assay. The cleaved caspase-12 expression was gradually increased with age in both WT mice ($n = 6$; $t = 6.280$, $P < 0.01$ and $t = 2.625$, $P < 0.05$, for 7- and 12-month-old mice vs. 2-month-old ones, respectively) and 5×FAD

mice ($n = 6$, $t = 3.320$, $P < 0.05$, $t = 3.427$, $P < 0.05$ for 7- and 12-month-old mice vs. 2-month-old ones, respectively). Of note, caspase-12 activation was higher in 5×FAD mice at 2-, 7-, and 12-month-old when compared with the activation status observed in WT mice. This increase was significant at 2 and 7 months of age ($n = 6$, $t = 5.365$, $P < 0.01$ for 2-month-old mice; $t = 2.869$, $P < 0.05$ for 7-month-old mice) [Figure 3b].

A recent study has reported that the p38 pathway is simultaneously activated to promote CHOP transcription to induce cell apoptosis.^[13] However, it remains unknown if JNK signaling is activated to trigger CHOP. The present data displayed that p-JNK/JNK increased mildly in 5×FAD mice at 2- and 12-month-old when in comparison with the levels detected in WT mice although the increase was not statistically different. These observations indicate that cell apoptosis in 5×FAD mice is not dependent on the JNK pathway [Figure 3c].

Taken together, these data suggest that ERS-specific CHOP and cleaved caspase-12 are sustainably upregulated in 5×FAD mice.

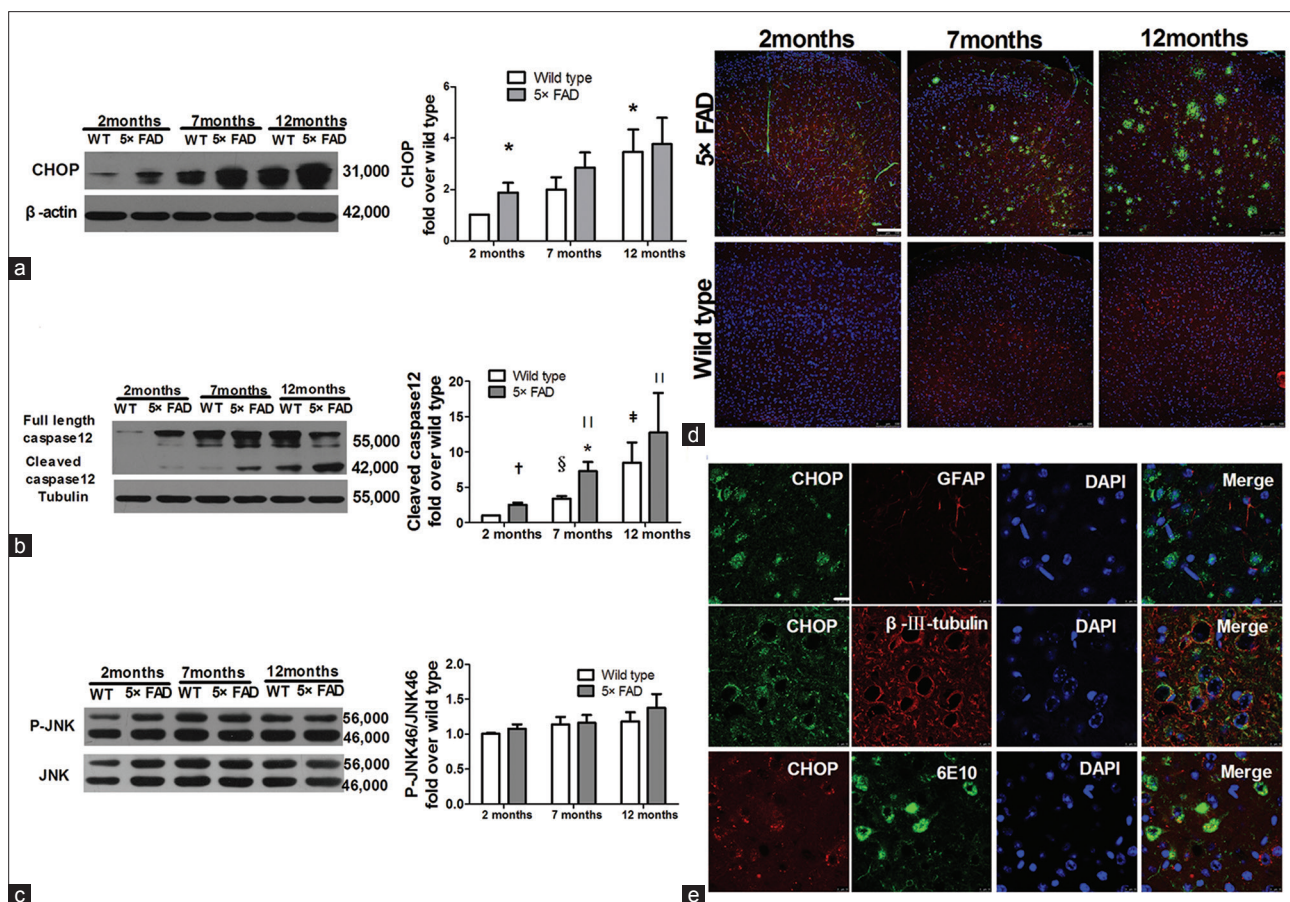


Figure 3: Significant increase of pro-apoptotic factors, CHOP and cleaved caspase-12 in 5×FAD mice. (a) Western blots analyses revealed that CHOP protein increased with age in 5×FAD mice ($n = 7$, $*P < 0.05$ vs. 2-month WT mice). (b) Western blots analysis showed that caspase-12 activation increased with age in 5×FAD mice ($n = 6$, $*P < 0.05$, $†P < 0.01$ vs. age-matched WT mice; $‡P < 0.05$, $§P < 0.01$ vs. 2-month WT mice; $||P < 0.05$ vs. 2-month 5×FAD mice). (c) Western blots analysis showed the expression of p-JNK/JNK. (d) Confocal images of CHOP (red), 6E10 (A β , green) and nuclei (DAPI, blue) in the cortical slices of 2-, 7-, and 12-month-old mice by immunofluorescence staining. Scale bars = 100 μ m. (e) Confocal images of CHOP (green), GFAP (red) or β -III-tubulin (red) in the frontal cortical slices of 7-month-old 5×FAD mice by immunofluorescent staining. The bottom row of (e) indicates immunofluorescent staining of CHOP (red) and 6E10 (green, targeting A β). Scale bars = 10 μ m. 5×FAD: Transgenic mice with five familial Alzheimer's disease; WT: Wild-type mice; CHOP: CCAAT/enhancer-binding protein homologous protein; JNK: c-Jun amino-terminal kinase; A β : Amyloid β ; 6E10: The antibody targeting A β ; GFAP: Glial fibrillary acidic protein; DAPI: 6-diamidino-2-phenylindole.

DISCUSSION

In 5×FAD mice, we observed that neuronal loss and cleaved caspase-3 increase at the age of 12 months, cognitive deficit at the age of 7 months and 12 months. Interestingly, at the age of 2-month-old 5×FAD mice, the related factors involved in the ERS-associated UPR pathway, including CHOP, cleaved caspase-12, GRP 78, and SYVN1, were significantly increased compared with those in age-matched WT mice. These findings suggest that 2-month-old 5×FAD mice exhibit enhanced ERS-associated UPR pathway, consistent with intracellular A β aggregation in neurons.

Oakley *et al.*^[10] reported, in 5×FAD brain, accumulated intraneuronal A β_{42} starting at 1.5 months of age, the presence of cerebral amyloid plaques and gliosis at 2 months of age, decreased synaptic markers including synaptophysin and postsynaptic density 95 (PSD95) accompanied by cognition deficit at 4 months of age, and pyramidal neuron loss in

cortical layer 5 at 9 months of age. Consistently, in our study, the deposit of intra- and extra-neuronal A β increased with age in 5×FAD brain; neuronal loss in cortical layer 5 was observed at 12 months of age; however, before significant neuron loss, impaired memory of 5×FAD mice at 7 months of age was monitored in the Morris water maze. Our previous study^[14,15] has also shown that cognitive impairment present in 5×FAD mice was accompanied by structural degradation of synapses and decreased expression of synaptophysin and PSD95 in the brain at the age of 6–7 months.

Under physiological conditions, approximately one-third of proteins in the ER are assembled abnormally and do not form mature proteins. Aberrant proteins are bound by chaperone proteins, such as GRP 78, to be repaired or transported into the ER-associated ubiquitin-proteasome system for degradation via the ERAD pathway, which serves as an accurate quality control system.^[16] ERAD promotes the interaction between ubiquitin and proteins waiting for

degradation via E1, E2, and E3. Ubiquitin-labeled proteins are subsequently degraded by the 26S proteasome. An impaired proteasome system leads to accumulation of aberrant proteins and increased risk of cell death.^[17] Sustained ERS induces the activation of the ER-specific apoptosis pathway by promoting the expression of CHOP and caspase-12 activation. ERS characterized by increased ERS-specific apoptosis is obvious in postmortem examinations of brain tissues of AD patients.^[18-20] *In vitro* experiments have also confirmed that A β induces the cellular ERS response directly,^[21,22] indicating that abnormal aggregation of A β is responsible for ERS induction.^[23-25] Other studies have shown that astrocytes and macrophages also induce ERS.^[26,27] However, in our study, the co-immunostaining of GRP 78 and CHOP with astrocytic or neuronal markers showed that ERS in cortical tissues occurred mainly in neurons. Therefore, the ERS-associated proteins examined here represent neuronal ERS and reveal the impact of the UPR on neuronal functions under A β -induced stress conditions.

In this study, we selected mice at 2, 7, and 12 months of age to investigate the changes of ERS-associated proteins in 5 \times FAD mice and WT mice. Our results showed that the expression of GRP 78 and SYVN1 changed without statistical significance but displayed an early-increase and subsequent-decline tendency from 2 to 12 months in WT mice. Interestingly, at the age of 2 months, the expression

of GRP 78 and SYVN1 in 5 \times FAD brains was significantly higher than that in WT mice; however, at the age of 12 months, GRP 78 level in 5 \times FAD brains significantly declined when compared with that of 2-month-old 5 \times FAD mice. Meanwhile, the expression of CHOP and cleaved caspase-12 increased continuously with age, either in 5 \times FAD mice or in WT mice. Of note, the level of CHOP and cleaved caspase-12 in 5 \times FAD mice was obviously higher than that in WT mice. Altogether, we speculate that A β in 2-month-old 5 \times FAD brains lead to higher ERS level than that of WT mice, which produces a cellular protective effect, on the one hand, up-regulating the expression of ER chaperones and related degradation proteins mainly via pIRE1 α -XBP1s and ATF6 α pathways at the early stage of AD to eliminate A β ; on the other hand, inducing increased expression of downstream signaling pathways molecules, especially pro-apoptotic proteins (cleaved caspase-12 and CHOP). Interestingly, no significant differences in pJNK/JNK levels were found between 5 \times FAD mice and WT mice at different periods, which indicates that the pJNK/JNK pathway is not involved in A β -induced ERS. Under sustained stress conditions caused by the A β -associated toxic effects, the protective function of the UPR declines and the pro-apoptotic functions are enhanced gradually. The pro-apoptotic functions of the UPR may lead to functional impairment of neurons and even death [Figure 4].

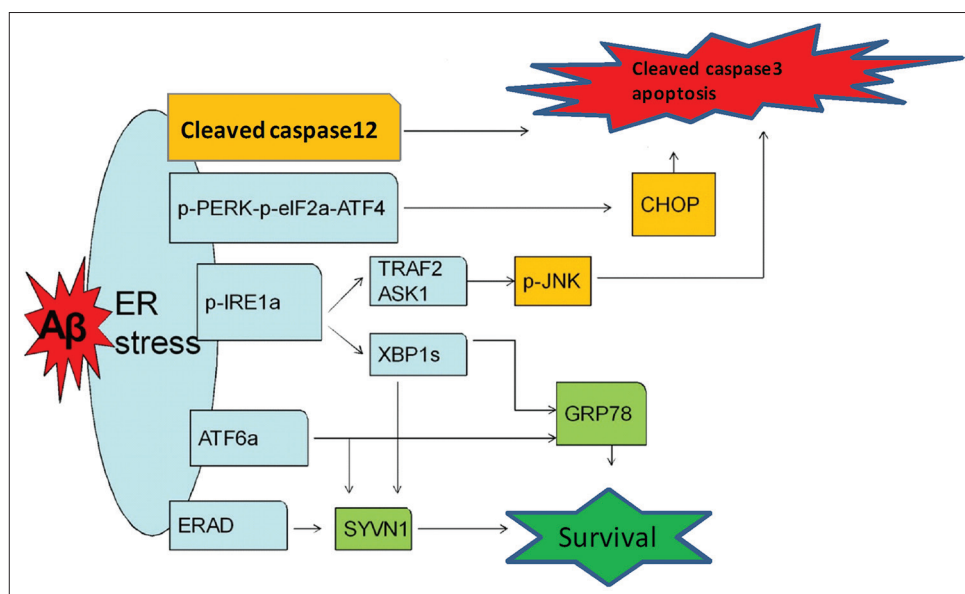


Figure 4: Schematic drawing shows that activated UPR pathways of ERS induced by intraneuronal β -amyloid in 5 \times FAD mice. A β in 2-month-old 5 \times FAD brains lead to higher ERS level than that of WT mice, which produces a cellular protective effect, on the one hand, up-regulating the expression of ER chaperones and related degradation proteins mainly via p-IRE1 α -XBP1s and ATF6 α pathways at the early stage of AD to eliminate A β ; on the other hand, inducing increased expression of downstream signaling pathways molecules, especially pro-apoptotic proteins (cleaved caspase-12 and CHOP). Under sustained stress conditions caused by the A β -associated toxic effects, the protective function of the UPR declines and the pro-apoptotic functions are enhanced gradually. The pro-apoptotic functions of the UPR may lead to functional impairment of neurons and even death. UPR: Unfolded protein response; ERS: Endoplasmic reticulum stress; A β : Amyloid β ; 5 \times FAD: Transgenic mice with five familial Alzheimer's disease; p-PERK: Phosphorylated protein kinase RNA-like ER kinase; p-eIF2 α : Phosphorylated eukaryotic translation initiation factor 2 α ; ATF4: Activating transcription factor 4; CHOP: CCAAT/enhancer-binding protein homologous protein; p-IRE-1 α : Phosphorylated inositol-requiring enzyme 1 α ; XBP1s: Spliced X box-binding protein 1; ATF6 α : Activating transcription factor 6 α ; GRP 78: Glucose-regulated protein 78; ERAD: Endoplasmic reticulum-associated protein degradation; SYVN1: Ubiquitin ligase synovial apoptosis inhibitor 1; TRAF2: Tumor necrosis factor-receptor-associated factor 2; ASK1: Apoptosis signal-regulating kinase 1; JNK: c-Jun amino-terminal kinase.

In conclusion, current data reveal that intracellular A β aggregation induces obvious ERS in neurons at the early stage of 5 \times FAD brains. Imbalanced regulation of GRP 78 or SYVN1 and CHOP or cleaved caspase-12 may be involved in the resistance to the restoration of ER homeostasis in A β -secreting neurons. If the development of ERS can be delayed or reduced appropriately or the protective functions of the UPR can be enhanced exogenously, the capacity of the ER to tolerate abnormal proteins can be increased to delay cell damage and disease progression. Targeting at ERS to control the pathophysiological changes at the early stage of AD may be a better strategy for the prevention and treatment of AD.

Acknowledgment

We would like to thank Prof. Marry Jo Ladu (Department of Anatomy and Cell Biology, University of Illinois at Chicago, USA) for providing the 5 \times FAD mice.

Financial support and sponsorship

This work was supported by grants from the National Natural Science Foundation of China (No. 91232709, No. 811171216, and No. 81161120496 for Prof. Xiao-Chun Chen, and No. 81200991 for Prof. Xiao-Dong Pan) and the National and Fujian Province's Key Clinical Specialty Discipline Construction Programs.

Conflicts of interest

There are no conflicts of interest.

REFERENCES

1. Tanzi RE, Bertram L. Twenty years of the Alzheimer's disease amyloid hypothesis: A genetic perspective. *Cell* 2005;120:545-55. doi: 10.1016/j.cell.2005.02.008.
2. Yoshida H. ER stress and diseases. *FEBS J* 2007;274:630-58. doi: 10.1111/j.1742-4658.2007.05639.x.
3. Ron D, Walter P. Signal integration in the endoplasmic reticulum unfolded protein response. *Nat Rev Mol Cell Biol* 2007;8:519-29. doi: 10.1038/nrm2199.
4. Kim I, Xu W, Reed JC. Cell death and endoplasmic reticulum stress: Disease relevance and therapeutic opportunities. *Nat Rev Drug Discov* 2008;7:1013-30. doi: 10.1038/nrd2755.
5. Paschen W, Mengesdorf T. Endoplasmic reticulum stress response and neurodegeneration. *Cell Calcium* 2005;38:409-15. doi: 10.1016/j.ceca.2005.06.019.
6. Kaufman RJ. Orchestrating the unfolded protein response in health and disease. *J Clin Invest* 2002;110:1389-98. doi: 10.1172/jci16886.
7. Bertolotti A, Zhang Y, Hendershot LM, Harding HP, Ron D. Dynamic interaction of BiP and ER stress transducers in the unfolded-protein response. *Nat Cell Biol* 2000;2:326-32. doi: 10.1038/35014014.
8. Su H, Wang X. The ubiquitin-proteasome system in cardiac proteinopathy: A quality control perspective. *Cardiovasc Res* 2010;85:253-62. doi: 10.1093/cvr/cvp287.
9. Kalai M, Lamkanfi M, Denecker G, Boogmans M, Lippens S, Meeus A, *et al.* Regulation of the expression and processing of caspase-12. *J Cell Biol* 2003;162:457-67. doi: 10.1083/jcb.200303157.
10. Oakley H, Cole SL, Logan S, Maus E, Shao P, Craft J, *et al.* Intraneuronal beta-amyloid aggregates, neurodegeneration, and neuron loss in transgenic mice with five familial Alzheimer's disease mutations: Potential factors in amyloid plaque formation. *J Neurosci* 2006;26:10129-40. doi: 10.1523/jneurosci.1202-06.2006.
11. Vorhees CV, Williams MT. Morris water maze: Procedures for assessing spatial and related forms of learning and memory. *Nat Protoc* 2006;1:848-58. doi: 10.1038/nprot.2006.116.
12. Cao Y, Hao Y, Li H, Liu Q, Gao F, Liu W, *et al.* Role of endoplasmic reticulum stress in apoptosis of differentiated mouse podocytes induced by high glucose. *Int J Mol Med* 2014;33:809-16. doi: 10.3892/ijmm.2014.1642.
13. Jiang Q, Li F, Shi K, Wu P, An J, Yang Y, *et al.* ATF4 activation by the p38MAPK-eIF4E axis mediates apoptosis and autophagy induced by selenite in Jurkat cells. *FEBS Lett* 2013;587:2420-9. doi: 10.1016/j.febslet.2013.06.011.
14. Zeng Y, Zhang J, Zhu Y, Zhang J, Shen H, Lu J, *et al.* Triphenylolide improves cognitive deficits by reducing amyloid β and upregulating synapse-related proteins in a transgenic model of Alzheimer's disease. *J Neurochem* 2015;133:38-52. doi: 10.1111/jnc.13056.
15. Zheng K, Dai X, Xiao N, Wu X, Wei Z, Fang W, *et al.* Curcumin ameliorates memory decline via inhibiting BACE1 expression and β -amyloid pathology in 5 \times FAD transgenic mice. *Mol Neurobiol* 2016. doi: 10.1007/s12035-016-9802-9.
16. Ellgaard L, Helenius A. Quality control in the endoplasmic reticulum. *Nat Rev Mol Cell Biol* 2003;4:181-91. doi: 10.1038/nrm1052.
17. Gorman AM. Neuronal cell death in neurodegenerative diseases: Recurring themes around protein handling. *J Cell Mol Med* 2008;12:2263-80. doi: 10.1111/j.1582-4934.2008.00402.x.
18. Hoozemans JJ, Veerhuis R, Van Haastert ES, Rozemuller JM, Baas F, Eikelenboom P, *et al.* The unfolded protein response is activated in Alzheimer's disease. *Acta Neuropathol* 2005;110:165-72. doi: 10.1007/s00401-005-1038-0.
19. Hamos JE, Oblas B, Pulaski-Salo D, Welch WJ, Bole DG, Drachman DA. Expression of heat shock proteins in Alzheimer's disease. *Neurology* 1991;41:345-50.
20. Unterberger U, Höftberger R, Gelpi E, Flicker H, Budka H, Voigtländer T. Endoplasmic reticulum stress features are prominent in Alzheimer disease but not in prion diseases *in vivo*. *J Neuropathol Exp Neurol* 2006;65:348-57. doi: 10.1097/01.jnen.0000218445.30535.6f.
21. Cook DG, Forman MS, Sung JC, Leight S, Kolson DL, Iwatsubo T, *et al.* Alzheimer's A beta(1-42) is generated in the endoplasmic reticulum/intermediate compartment of NT2N cells. *Nat Med* 1997;3:1021-3.
22. Chafekar SM, Hoozemans JJ, Zwart R, Baas F, Scheper W. A beta 1-42 induces mild endoplasmic reticulum stress in an aggregation state-dependent manner. *Antioxid Redox Signal* 2007;9:2245-54. doi: 10.1089/ars.2007.1797.
23. Umeda T, Tomiyama T, Sakama N, Tanaka S, Lambert MP, Klein WL, *et al.* Intraneuronal amyloid β oligomers cause cell death via endoplasmic reticulum stress, endosomal/lysosomal leakage, and mitochondrial dysfunction *in vivo*. *J Neurosci Res* 2011;89:1031-42. doi: 10.1002/jnr.22640.
24. Tomiyama T, Matsuyama S, Iso H, Umeda T, Takuma H, Ohnishi K, *et al.* A mouse model of amyloid beta oligomers: Their contribution to synaptic alteration, abnormal tau phosphorylation, glial activation, and neuronal loss *in vivo*. *J Neurosci* 2010;30:4845-56. doi: 10.1523/jneurosci.5825-09.2010.
25. Huang HC, Tang D, Lu SY, Jiang ZF. Endoplasmic reticulum stress as a novel neuronal mediator in Alzheimer's disease. *Neurol Res* 2015;37:366-74. doi: 10.1179/1743132814y.0000000448.
26. Zhong N, Ramaswamy G, Weisgraber KH. Apolipoprotein E4 domain interaction induces endoplasmic reticulum stress and impairs astrocyte function. *J Biol Chem* 2009;284:27273-80. doi: 10.1074/jbc.M109.014464.
27. Cash JG, Kuhel DG, Basford JE, Jaeschke A, Chatterjee TK, Weintraub NL, *et al.* Apolipoprotein E4 impairs macrophage efferocytosis and potentiates apoptosis by accelerating endoplasmic reticulum stress. *J Biol Chem* 2012;287:27876-84. doi: 10.1074/jbc.M112.377549.